Numerical investigation of external electromagnetic field induced on Organic Solar Cells model using FEM Analysis

Grazia Lo Sciuto

Department of Electrical, Electronic and Informatics Engineering
University of Catania (*Italy*)
glosciuto@dii.unict.it

Abstract—**Research on photovoltaic energy conversion has recently received great impulse due to the growing demand for low carbon dioxide emission energy sources. In particular, the high manufacturing cost of crystalline silicon and the latest advancements on semiconducting polymer design and synthesis in recent years have directed the attention of the scientific community towards Organic Solar Cells (OSCs). In this paper, the electromagnetic field induced on OSCs has been investigated to evaluate the potential of the optical efficiecy at several frequencies of OSCs.**

Index Terms—**FEM; Organic solar cells; Electromagnetic field**

I. INTRODUCTION

The electronic devices more efficient and economics able to work as solar cells can be developed using several types of material with different structural architectures [1], [2]. The detailed research on the fullerene properties could represent the keystone for the diffusion of the organic solar cells. The organic based solar cells are nothing new, but the major constraint of this innovation lies in his basic constituent, the fullerene, too expensive for a mass dissemination. To increase the knowledge of the fullerene has enabled to develop other low-cost alternatives. It is a mixture of polymers capable of producing structural and electronic changes in the photovoltaic cells such as tripling the efficiency. Scientists have embedded in the active layer of the solar cells, based on carbon, the pure graphene with surprising results: the conductivity is increased and the efficiency of photovoltaic cells has grown of the 200% in energy systems. Unlike solar cells based on silicon or germanium existing in the market, the polymers are less expensive and more malleable. The polymer solar cells can be folded like a sheet and carried easily.

In order to be competitive for the production of solar energy on an industrial scale, this technology must however dissolve a crucial node. Compared to inorganic semiconductors, the organic materials have a lower charge transfer coefficient, namely the electron transfer speeds in the energy system. Although thinner and flexible, the organic photovoltaic films fail to capture an equally large portion of the solar spectrum with a lower amount of energy based on the silicon technologies.

However, the mechanical reliability of full cell packaging is rarely concerned. As solar cell often appears to be a part

of structure, stress will inevitably act on the package [3], [4], [5], [6].

The researchers have tried to solved these problems by increasing the ability to transport electrons polymer using polymer mixture, studying the morphology of the organic photovoltaic and new solutions to increase the charge transfer coefficient. During the last years the development of organic photovoltaics (OPV) focuses on inexpensive materials, promising a simple processing and integration on different substrates with high performance. In this regard the equivalent circuit modeling of photovoltaic devices can be useful for understanding the performance and the optimization of the design solar cells [7], developing faster algorithms and computational techniques without costly experiments, although it is characterized by a very high level of abstraction. Since the basic equivalent circuit model is represented by ideal circuit element such as diode, current source and resistance to understand and calculate the $J-V$ characteristics of inorganic solar cells.

Doo-Hyun Ko et al. [8] report organic solar cells with a photonic crystal geometry fabricated using a materials-agnostic process called PRINT wherein highly ordered arrays of nanoscale features are readily made in a single processing step over wide areas ($\approx 4\,cm^2$) that is scalable with the efficiency improvements of $\approx 70\%$ that result not only from greater absorption, but also from electrical enhancements [9]. Other authors present the efforts to enhance the stability of normal-geometry organic solar cells (n-OSCs), which are generally considered inferior to their inverted-geometry counterparts in terms of stability. The efficiency of organic solar cells is primarily limited by the active layer to absorb spectra. The active layer thickness varied between 95 to 115 nm [10]. Soo Jin Kim et al analyze the light trapping mechanism for a cell with a V-shape substrate configuration and demonstrate significantly improved photon absorption in an 5.3% efficient PCDTBT:PC70BM bulk heterojunction polymer solar cell. The measured short circuit current density improves by 29%, in agreement with model predictions, and the power conversion efficiency increases to 7.2%.

Thomas Rieks et al. [11] demonstrate a pathway for fully *roll-to-roll* (R2R) prepared organic solar cells in a normal geometry with a R2R sputtered aluminium top electrode,

optimizing the donor: acceptor ratio in the active layer the efficiency increased to 0.90%. So the normal geometry organic solar cells using a metal top contact can be produced using large scale production techniques [12].

Gholamhosain Haidari et al. [13] report on the simple fabrication of Ag NP films formed on indium tin oxide electrodes, coated with PEDOT:PSS and implemented into PCPDTBT:PC70BM solar cells, applying the finite-difference time-domain techniques to model the optical properties of different nanoparticle films and they demonstrate that the absorption and scattering efficiency of the particles are very sensitive to particle geometry [14], [15]. The author present an optical simulation of light management in Cu(In,Ga)Se2 thin-film solar cells with reduced absorber layer thickness, with the goal of absorption enhancement in the absorber layer [16]. The optical effects of an extra interfacial layer of poly (3,4-ethylenedioxythiophene)/(poly(styrenesulfonate) (PEDOT/PSS) on top of the ITO-electrode of a mono or multi-layer organic photovoltaic device, in which the incident light of sun is absorbed in the active layer is reported in [17].

From optical and electrical simulations, increasing the thickness of the organic solar cells device due to the low mobility of the organic materials, non-geminate recombination rate enhances and causes the power conversion efficiency reduction [18].

The optical performance of the P3HT:PCBM solar cell has been simulated by AMPS-1D to study the J -V characteristics and electric field with active layer thickness in [19].

The processes controlling the efficiency of hybrid planar devices comprising two semiconducting donor polymers and amorphous silicon,charge generation and the distribution of electric fields in a-Si:H/organic-hybrid solar cells have been investigated by [19], applying a transfer matrix formalism to model the absorption in the hybrid device including interference in the layer stackby.

By design and simulation of the OSCs devices is possible to provide a simple model for the performance analysis of extending the high frequency range. The electromagnetic field induced on solar devices has been investigated to evaluate the interactions of the optical model at several frequencies using as tool COMSOL to calculate the magnetic field effects starting from a sample with OSCs carried out in collaboration with Optoelectronic Organic Semiconductor Devices Laboratory (OOSDL), Department of Electrical and Computer Engineering Ben-Gurion University of the Negev, Israel.

II. The OSC Model

A bulk heterojunction solar cell consists of an active organic part with a donor and an acceptor material, the metal electrodes and the substrate. The substrate usually glass and transparent ensures that the light reaches the active material. The positive and negative electrodes respectively indium tin oxide and aluminum are responsible for the transport of the charges from the organic material to the electrical connections. The absorption of photons from incident light generates excitons namely bound electron-hole pairs, due to the stronger Coulomb
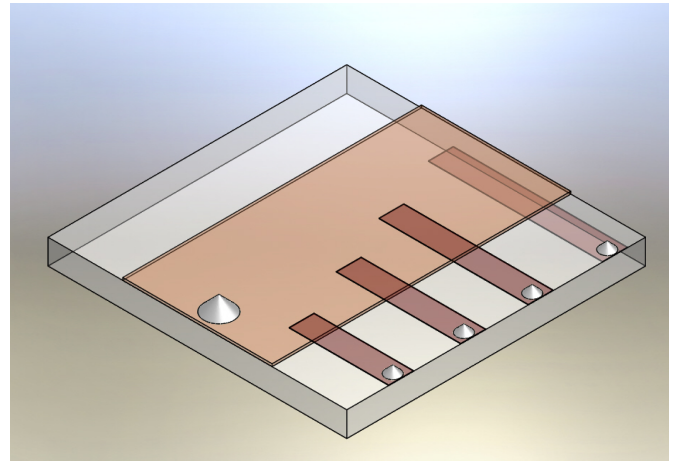

Fig. 1. 3D organic solar cell modeling in Solidworks

attraction in an organic materials. To generate electrical energy it is necessary to separate the charges to contribute to photocurrent in an organic cell. The exciton with a random process based on concentration gradients can diffuse at this donor/acceptor interface to dissociate and convert into free charge carriers, electrons and holes. To generate electrical energy it is necessary to separate the charges to contribute to photocurrent in an organic cell. The photons energy excites the electron from the HOMO to the LUMO band, where the HOMO and LUMO are equivalent to the valence band and conduction band known from classical physics. The exciton with a random process based on concentration gradients can diffuse at this donor/acceptor interface to dissociate and convert into free charge carriers, electrons and holes, when the interface is within the exciton diffusion length, typically is not very long some $10\,nm$ depending on the material in organic semiconductors. However excitons can recombine or decay back to the ground state, during the diffusion process before reaching the donor/acceptor interface, leading to absorbed photons that do not contribute to the current. In this case, the recombination rate depends on the charge density, as the probability of two charges meeting increases with higher carrier density. For an efficient exciton dissociation it has to be energetically favorable for the electron to be transferred to the LUMO of the acceptor or for the hole to the HOMO of the donor material, respectively. Finally, the charges due to an internal electric field and a gradient in the electrochemical potential are collected and transported towards the respective electrodes, electrons and holes can be extracted by cathode and anode, leading to current's generation to the external circuit [20], [21], [22], [23].

III. Materials and Fabrication

The procedure for fabrication of organic solar cell device is carried out inside the glovebox at low temperature $22\,C°$ compatible with their sensitivity and degradation very fast under normal air conditions, performed under a dry nitrogen atmosphere with an O_2 concentration of $1.7\,ppm$ and an
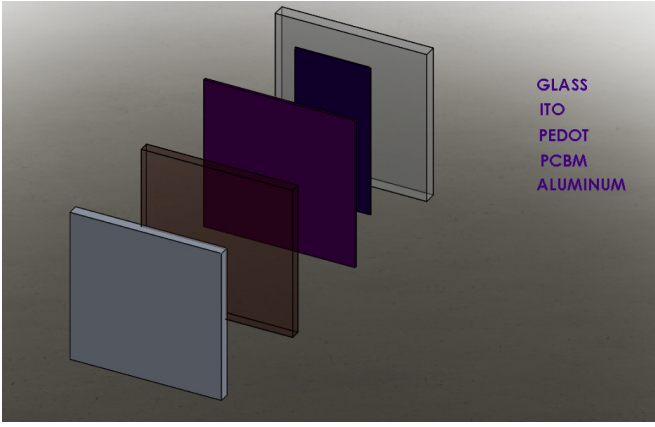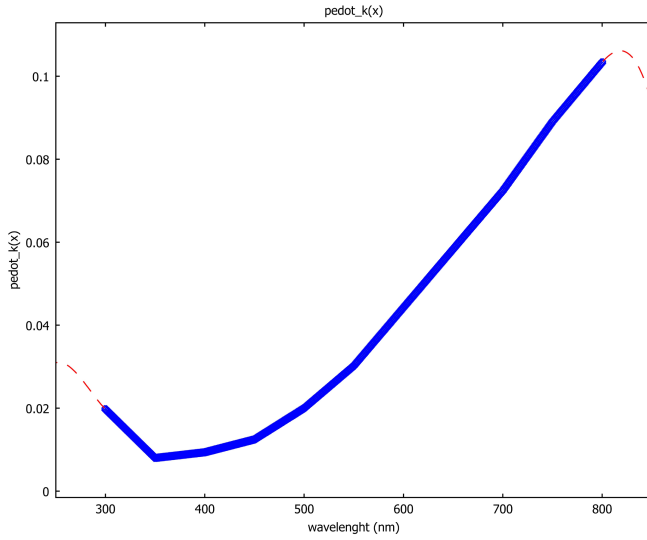
Fig. 2.   3D materials of OSC modeling in Solidworks

Fig. 3.   Extinction coefficient of Pedot

Fig. 4.   Refractive index of P3HT:PCBM blend

Fig. 5.   Extinction coefficient of P3HT:PCBM blend

H_2O concentration smaller than 0.1 ppm. The fabrication of polymer solar cells is based on four steps. Before the first step is the cleaning of ITO coated glass substrate to eliminate particles, contaminates and imperfections, in acetone, methanol and isopropanol bath for 15 minutes each one through an ultrasonic bath (53 kHz at room temperature). Afterwards the substrate is dipped into distilled water and put into a vacuum oven; the plasma cleaning need to remove of remaining oxygen molecules. The glass substrate is sized $12\,mm \times 12\,mm \times 0.7\,mm$ and is coated in the middle with a rectangular section $6\,mm \times 12\,mm$ and $90\,nm \pm 10\,nm$ of transparent thick ITO layer with resistance of $20\,Ohm/m^2$. The ITO is the anode with high transparency, conductivity but it is fragile and susceptible to deterioration. $PEDOT : PSS$ is a transparent conjugated polymer with thickness layer of 30 nm. Inside the glove box, a solution of *photo-active* polymer P3HT and PCBM is prepared. The P3HT:PCBM layer is deposited onto cleaned substrates by spin coating the samples at 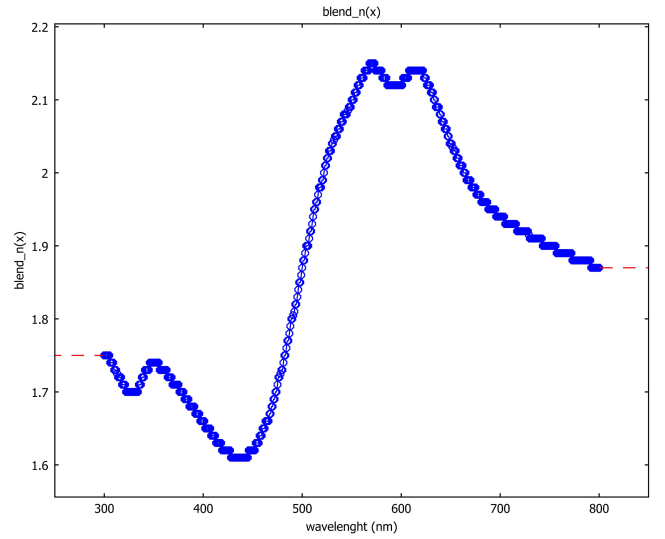$5000\,rpm$ (revolutions per minute) and an acceleration of $7000\,rpm/s$ for one minute, resulting in a layer thickness of approximately $200\,nm$. The acceptor material is the PCBM and P3HT is the donor material. Devices were completed by evaporation of aluminum $80\,nm$ in a vacuum, through a shadow mask used to create the preferred shape of aluminum cathodes.To connect the thin film to electrical wire the Silver Conductive Epoxy was deposited on small part of ITO removed locally and Aluminum layer.

IV. GEOMETRY

The model, shown in Figg. 1 and 2, consists of an embedded structure sample with domain size of $12 \times 12\,mm$ and layers thicknesses of: $80\,nm$ for metal electrode aluminum, $200\,nm$ of active layer pcbm, 30 nm of pedot: pss, $90\,nm$ of ITO and glass substrate with layer of $0.7\,mm$. The sample contains

Parameter	Value	Unit
ε_{air}	8.8590e-12	F/m
n_{air}	1	
n_{glass}	1	
λ	300 - 800	nm

four organic solar cells with different lengths, each of them has size of $4.50\,mm$, $5.50\,mm$, $6.50\,mm$ and $7.50\,mm$.

V. METHODOLOGY

It was presented an OSC simulated model in a large area of high frequency ($10^{14} - 3.75 * 10^{14}\,Hz$). The model is based on solving solves the Maxwell equation using the finite element method. The simulation electromagnetic effects in 2D and 3D were carried out within Comsol Multiphysics. The Maxwells equations in the time domain are:

$$\begin{aligned} \bigtriangledown \cdot D &= \rho \\ \bigtriangledown \times E &= -\partial_t B \\ \bigtriangledown \cdot B &= 0 \\ \bigtriangledown \times H &= J + \partial_t D \end{aligned}$$

Under varying assumptions, these equations are solved with a set of boundary conditions related to material for modeling perfect electrically conducting surfaces within the RF Module of COMSOL Multiphysics using the finite element method to solve for the electromagnetic fields within the modeling domains.

The optical properties of the organic thin lm materials such as $poly(3 - hexylthiophene) : poly(6,6 - phenylC61 - butyricacidmethylester)(P3HT : PCBM)andPEDOT : PSS/ITO$ are described by complex wavelength-dependent refraction index n. The values of the complex refractive indexes specified as a function of wavelength and used in the simulation were taken from the literature for P3HT, PCBM, ITO and Al. In Figg. 3, 4 and 5 are displayed the plots, as function of the wavelength, of the optical constants such as P3HT:PCBM and PEDOT in particular, the refractive index and the extinction coefficient are related by phisical materials properties. The refractive index of the environment is equal to the refractive index of air (n=1). In the table the optical and electrical values set used for the FEM analysis: The simulation was carried out at wavelengths in the range of absorption of the material. Then, parametric analysis of COMSOL was used with frequency as the changing parameter, ranging from 10^{14} Hz to $3.75 * 10^{14}$ Hz. The Perfectly matched layers (PMLs) are used to enclose the model domain. The methodology is consisted to define the equations to solve, creating the model geometry, define the material properties, setting up the boundaries. During the meshing step the model space has been discretized using finite elements. Solving a set of linear equations that describe the electric fields. The useful information are extracted from the computed electric and magnetic fields.
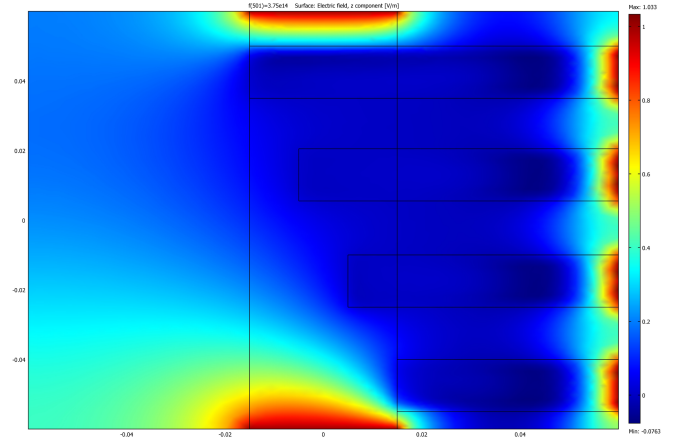

Fig. 6. Electic field in 2D, view from above of sample structure with OSCs

VI. CALCULATION AND RESULTS

An optical wave is propagated in the system determining the degradation of electric field amplitude due to interference by optical properties in each active layer. To better understand the interaction of the each OSCs, the simulation was repeated for a range of wavelength from 300 to 800 nm, where the incident light has an acceptable intensity on the optical models with different layers. The magnetic field distribution indicates the absorption of electromagnetic wave externally applied depending on the refractive index,wavelength and width of layers. The magnetic field is calculated on sample device with different OSCs located on top of the glass support. The structure and the electric field configuration, bidimensional and tridimensional, are represented in Fig. 6 and in Fig. 7 respectively.

As shown in Fig. 8, the magnetic field decrease along y axis illustrating the dependence with the layers and materials optical properties. Magnetic field results are reported in Fig. 9 for different OSCs, with the same trend. It is necessary to consider several different factors which affect the absorption of any organic photovoltaic device defined as number of photons absorption,exciton dissociaton. Therefore, more excitons are able to diffuse to the heterojunction and dissociate into free charges, moving to the electrodes where they are extracted and establish a photocurrent. An interesting extension to this work could be to examine and explore the relationship between efficiency and device thickness considering an ideal morphology organic solar cell.

VII. CONCLUSION

The results obtained by these simulations can promote to investigate the polymer materials attitudes examining a large range of frequencies and effects under external electric and magnetic field. An optical model relative to organic solar cells sample model is proposed by means the electromagnetic field simulation at large range of frequency. The simulations in this work were based upon finite element method with
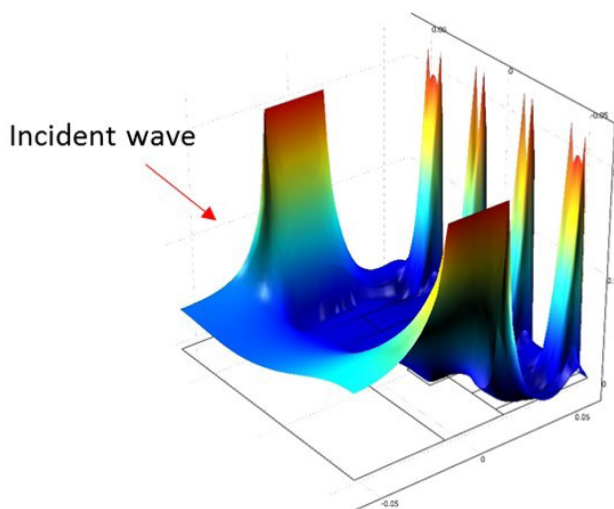
Fig. 7. 3D Surface plot of Electic field applied on sample structure with OSCs
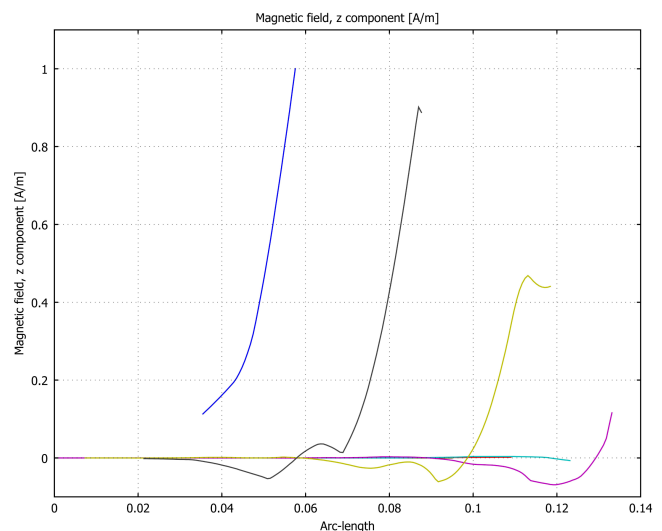

Fig. 9. Magnetic field of the sample containing the OSCs
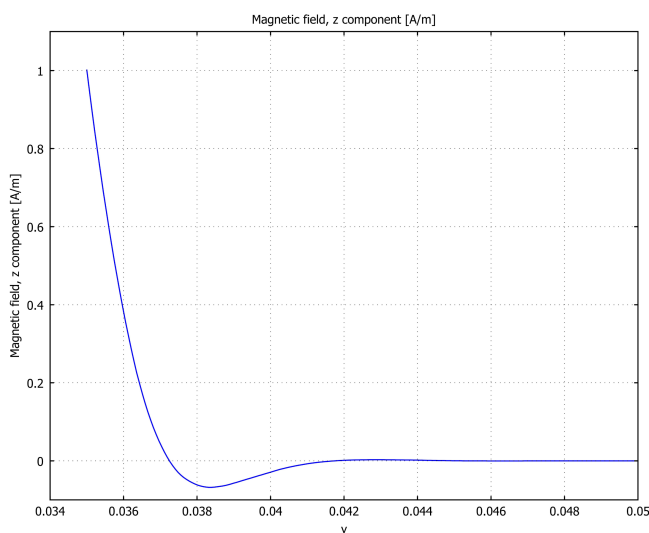

Fig. 8. Magnetic field of an organic solar cell

2D geometry. The simulations were carried out using the RF module of COMSOL Multiphysics software package

ACKNOWLEDGMENT

REFERENCES

[1] G. Capizzi, G. Lo Sciuto, C. Napoli, and E. Tramontana, "A multithread nested neural network architecture to model surface plasmon polaritons propagation," *Micromachines*, vol. 7, no. 7, 2016.

[2] D. Gotleyb, G. L. Sciuto, C. Napoli, R. Shikler, E. Tramontana, and M. Woźniak, "Characterisation and modeling of organic solar cells by using radial basis neural networks," in *International Conference on Artificial Intelligence and Soft Computing*. Springer, 2016, pp. 91–103.

[3] M. Calì and F. L. Savio, "Accurate 3d reconstruction of a rubber membrane inflated during a bulge test to evaluate anisotropy," in *Advances on Mechanics, Design Engineering and Manufacturing*. Springer, 2017, pp. 1221–1231.

[4] R. Damaševičius, C. Napoli, T. Sidekerskienė, and M. Woźniak, "Imf mode demixing in emd for jitter analysis," *Journal of Computational Science*, p. in press, 2017, dOI: 10.1016/j.jocs.2017.04.008.

[5] E. Pedulla, F. L. Savio, G. Plotino, N. M. Grande, S. Rapisarda, G. Gambarini, and G. La Rosa, "Effect of cyclic torsional preloading on cyclic fatigue resistance of protaper next and mtwo nickel–titanium instruments," *Giornale Italiano di Endodonzia*, vol. 29, no. 1, pp. 3–8, 2015.

[6] R. Damaševičius, C. Napoli, T. Sidekerskienė, and M. Woźniak, "Imf remixing for mode demixing in emd and application for jitter analysis," in *IEEE Symposium on Computers and Communication (ISCC)*. IEEE, 2016, pp. 50–55, dOI: 10.1109/ISCC.2016.7543713.

[7] F. Bonanno, G. Capizzi, G. L. Sciuto, D. Gotleyb, S. Linde, and R. Shikler, "Extraction parameters and optimization in organic solar cell by solving transcendental equations in circuital models combined with a neuroprocessing-based procedure," in *2016 International Symposium on Power Electronics, Electrical Drives, Automation and Motion (SPEEDAM)*, June 2016, pp. 872–877.

[8] D. Ko, J. Tumbleston, L. Zhang, S. Williams, J. Desimone, R. Lopez, and E. Samulski, *Photonic crystal morphology for organic solar cells*, 2009.

[9] D.-H. Ko, J. R. Tumbleston, L. Zhang, S. Williams, J. M. DeSimone, R. Lopez, and E. T. Samulski, "Photonic crystal geometry for organic solar cells," *Nano letters*, vol. 9, no. 7, pp. 2742–2746, 2009.

[10] W. J. Da Silva, F. K. Schneider, A. R. bin Mohd Yusoff, and J. Jang, "High performance polymer tandem solar cell," *Scientific reports*, vol. 5, p. 18090, 2015.

[11] T. Andersen, H. Dam, M. Hsel, M. Helgesen, J. Carl, T. Larsen-Olsen, S. Gevorgyan, J. Andreasen, J. Adams, N. Li, F. Machui, G. Spyropoulos, T. Ameri, N. Lematre, M. Legros, A. Scheel, D. Gaiser, K. Kreul, S. Berny, O. Lozman, S. Nordman, M. Vlimki, M. Vilkman, R. Sndergaard, M. Jrgensen, C. Brabec, and F. Krebs, "Scalable, ambient atmosphere roll-to-roll manufacture of encapsulated large area, flexible organic tandem solar cell modules," *Energy& Environmental Science*, vol. 7, pp. 2925–2933, 2014.

[12] T. R. Andersen, N. A. Cooling, F. Almyahi, A. S. Hart, N. C. Nicolaidis, K. Feron, M. Noori, B. Vaughan, M. J. Griffith, W. J. Belcher *et al.*, "Fully roll-to-roll prepared organic solar cells in normal geometry with

a sputter-coated aluminium top-electrode," *Solar Energy Materials and Solar Cells*, vol. 149, pp. 103–109, 2016.

[13] G. Haidari, M. Hajimahmoodzadeh, H. R. Fallah, A. Peukert, A. Chanaewa, and E. von Hauff, "Thermally evaporated ag nanoparticle films for plasmonic enhancement in organic solar cells: effects of particle geometry," *physica status solidi (RRL) Rapid Research Letters*, vol. 9, no. 3, pp. 161–165, 2015.

[14] R. Damaševičius, R. Maskeliūnas, V. A., and M. Woźniak, "Smartphone user identity verification using gait characteristics," *Symmetry*, vol. 8, no. 10, pp. 100:1–100:20, 2016.

[15] R. Damaševičius, M. Vasiljevas, J. Salkevicius, and M. Woźniak, "Human activity recognition in aal environments using random projections," *Computational and Mathematical Methods in Medicine*, vol. 2016, pp. 4 073 584:1–4 073 584:17, 2016.

[16] G. Haidari, M. Hajimahmoodzadeh, H. R. Fallah, A. Peukert, A. Chanaewa, and E. Hauff, "Thermally evaporated ag nanoparticle films for plasmonic enhancement in organic solar cells: effects of particle geometry," *physica status solidi (RRL)-Rapid Research Letters*, vol. 9, no. 3, pp. 161–165, 2015.

[17] M. M. Boudia and A. Cheknane, "A modelling and simulation approach of electromagnetic field in organic photovoltaic devices," *World Journal of Modelling and Simulation*, vol. 6, no. 3, pp. 198–204, 2010.

[18] M. Farrokhifar, A. Rostami, and N. Sadoogi, "Opto-electrical simulation of organic solar cells," in *Modelling Symposium (EMS), 2014 European*. IEEE, 2014, pp. 507–512.

[19] N. Singh, A. Chaudhary, and N. Rastogi, "Simulation of organic solar cell at different active layer thickness," *International Journal of Material Science*, 2015.

[20] F. Famoso, R. Lanzafame, S. Maenza, and P. Scandura, "Performance comparison between low concentration photovoltaic and fixed angle pv systems," vol. 81, 2015, pp. 516–525.

[21] C. Napoli, G. Pappalardo, G. M. Tina, and E. Tramontana, "Cooperative strategy for optimal management of smart grids by wavelet rnns and cloud computing," *IEEE transactions on neural networks and learning systems*, vol. 27, no. 8, pp. 1672–1685, 2016.

[22] F. Famoso, R. Lanzafame, S. Maenza, and P. Scandura, "Performance comparison between micro-inverter and string-inverter photovoltaic systems," vol. 81, 2015, pp. 526–539.

[23] S. Brusca, R. Lanzafame, and M. Messina, "Flow similitude laws applied to wind turbines through blade element momentum theory numerical codes," *International Journal of Energy and Environmental Engineering*, vol. 5, no. 4, pp. 313–322, 2014.